ANALYSIS OF TURNING MOTION FOR DEVELOPING A BUTTERFLY-STYLE FLAPPING ROBOT

YUTA OZAWA[1], TARO FUJIKAWA[2], KOKI KIKUCHI[1]

[1]Chiba Institute of Technology
The department of Advanced Robotics
Chiba, Japan
[2]Tokyo Denki University
The department of Robotics and Mechatronics
Tokyo, Japan
DOI: 10.17973/MMSJ.2018_03_201765
e-mail: kikut@ieee.org

In this study, to achieve turning flight of a butterfly-style flapping robot, we first analyzed the flight of a butterfly and then performed flight experiments using flapping robots. Flight analysis of a butterfly revealed difference between the left and right lead-lag angles during yaw turning flight. Based on analysis result, the two cases of flight experiment were performed in terms of the rotational direction of an actuator and the symmetry of swept-forward angle. The rotational direction of the actuator affected the posture for even the flapping robot with the symmetric wings. On the other hand, the flapping robot with the asymmetric swept-forward angles of 10° changed the roll and yaw angles by 18.8° and 28.8°. These results revealed that the asymmetric swept-forward angles generated roll and yaw moments compensating the effect by the rotational direction of the actuator and turned the robot.

KEYWORDS

small flapping robot, butterfly, turning flight, asymmetric wings, swept-forward angle, rotational direction of an actuator

1 INTRODUCTION

Since flapping flight is a flight mode that is often used in nature and enables versatile flight motions such as sharp turns, vertical takeoff, and hovering, numerous flapping robots have been studied [Yokoyama 2008, Hsiao 2012, Karasek 2016, Lui 2012]. This flight mode has different characteristics depending on the scale of living creatures. Large-scale species, such as hawks and eagles, ascend using the air bump phenomenon and fly mainly by gliding. On the other hand, small-scale species, such as hummingbirds and butterflies, fly agilely using only flapping flight without exploiting the air bump phenomenon. For this reason, various small-scale flapping robots, and particularly, insect-scale flapping robots, have been developed. [Wood 2008] developed a fly-scale robot using piezoelectric element and achieved vertical flight. [Hu 2009] fabricated artificial dragonfly wings and analyzed the lift and thrust when the fore and hind wings flap with a phase difference. Moreover, although they developed a dragonfly-style robot, its flapping frequency was approximately 7 Hz, which is lower than that of a real dragonfly. These robots have not yet achieved practical autonomous flight, because it is difficult to reproduce the flapping frequency and many degrees of freedom (DOFs) of the wings involved in motions such as lead-lag, feathering, and flapping motions. For example, the flapping frequency of a fly or a bee exceeds 100 Hz, which is extremely difficult to achieve without a heavy motor system consisting of gears, a motor, a driver, and an external power supply. Moreover, since the dragonfly has four wings, which perform not only flapping, but also lead-lag and feathering, the dragonfly-style robot requires many actuators and a complex link mechanism. However, it makes the motion control complex and increases the dissipation by link friction. As a result, the flight performance deteriorates.

To overcome such challenges, we have developed a butterfly-style flapping robot with a mass of 500 mg and a wingspan of 120 mm [Fujikawa 2010, Udagawa 2005]. This robot has a low flapping frequency of 10 Hz, reproduced flapping, lead-lag, and abdomen swinging motions with only one DOF, and achieves stepwise flight with nose up and nose down motions (i.e., changing the pitch posture periodically) similar to a butterfly. Furthermore, we have analyzed the mechanism of the pitch posture control using the flapping robot and clarified that the pitch posture was controlled by the position balance between the center of mass and the swept-forward angle [Fujikawa 2009]. From this, in this study, we analyze the turning flight (i.e., the rotation around the yaw axis) of a butterfly and investigate the parameters affecting the turning flight. We then focus on the obtained dominant parameters and clarify the relationship with the straightness characteristic using the flapping robot. Finally, we implement the obtained mechanism for the flapping robot and demonstrate the turning flight experimentally.

The remainder of this paper is organized as follows. In Section 2, we analyze the turning flight of a butterfly. In Section 3, we describe the developed butterfly-style flapping robot and an experiment on turning flight conducted using the flapping robot. Finally, in Section 4, we conclude this paper and outline future work.

2 TURNING CHARACTERISTICS OF A BUTTERFLY

To investigate the flight parameters affecting the turning flight, we analyzed the flight motion of a swallowtail butterfly (*Papilio xuthus*) based on the images obtained by a 3D high-speed camera system consisting of x, y, and z cameras [Shindo 2014]. Figure 1 and Table 1 show the specification of examined butterflies. The camera (DITECT: HAS-D3) had a frame rate of 1000 fps, a shutter speed of 1/5000 s, and an image resolution of 1280×1024 pixels. Figure 2 illustrates the definitions of the flight parameters. The posture of a butterfly is expressed by roll, pitch, and yaw angles, i.e., X_B, Y_B, and Z_B axis rotations. The angle between the spanwise direction (Y_B) and the leading edge line of the forewing is referred to as the swept-forward angle if the angle is positive, whereas this angle is referred to as the sweepback angle if the angle is negative. In this study, we use the lead-lag angle. The radius of curvature of the flight trajectory is positive when a butterfly turns left.

Based on the above conditions, we photographed and analyzed three times the forward and turning flights of a butterfly during one stroke (approximately 100 ms), respectively. Figures 3 and 4 show stroboscopic images (as viewed from above the X-Y plane) of the forward and turning flights of a butterfly. The trajectory of the thorax, the body vector, and the velocity vector indicate that the butterfly first changed its yaw posture and then gradually changed its traveling direction. Figure 5 shows thorax trajectories on the X-Y plane for the forward and turning flights that the initial yaw angles corresponded and Figs. 6 and 7 indicate the stroke histories of roll and yaw angles, respectively. While the radius of curvature of forward flight was -730 mm (-13.8 body length), that of the turning flight was -52 mm (-1.0 body length). Hence, the radius of curvature of the turning flight was close to the

body length. Note that the smaller the radius of curvature, the sharper the turn. The value of 0 means the pivot turn. The roll angles for the forward and turning flights varied by 12.2° and 33.6°, respectively (Fig. 6). The difference was 21.4°. On the other hand, the yaw angles for the forward and turning flights varied by 10.2° and 71.1°, respectively (Fig. 7). The difference was 60.9°. Table 2 shows the relationship between the radius of curvature and the roll and yaw posture for forward and turning flights. The radius of curvature and the roll angle had negative correlation (correlation coefficient: r=-0.50) and the radius of curvature and the yaw angle had strong negative correlation (r=-0.72). The roll and yaw angles had very strong positive correlation (r=0.87). These results indicate that the turning flight of a butterfly was generated by a combination of the roll and yaw angles. Figures 8 and 9 show the stroke histories of the lead-lag angles. While no difference was found between the left and right lead-lag angles during the forward flight, the average difference of 6.9° was observed during the turning flight. Table 3 shows the obtained difference between the left and right lead-lag angles of butterflies. These results showed that there was high possibility that a butterfly realized the turning flight by breaking the symmetry of left and right lead-lag angles. Hence, a butterfly increased the right lead-lag angle during left turn and the left lead-lag angle during right turn. Based on these results, we focus on the difference between the left and right lead-lag angles, i.e., asymmetric wing control, and investigate the relationship between the posture and the asymmetric wings in a flight experiment using the fabricated flapping robot.

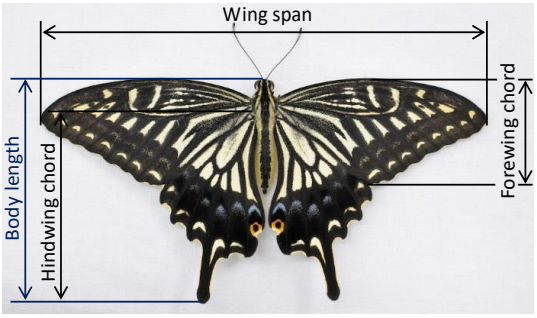

Figure 1. Overview of a swallowtail butterfly

Butterfly	Wing span [mm]	Forewing chord [mm]	Hindwing chord [mm]	Body length [mm]
1	104	23	49	53
2	103	23	43	50
3	105	32	40	46
4	118	27	45	52
5	110	29	49	57
6	110	27	53	61

Table 1. Specification of butterflies

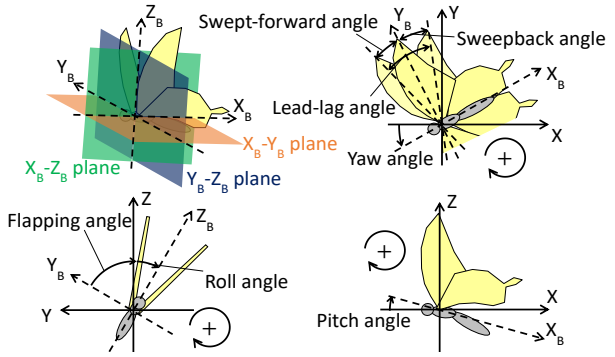

Figure 2. Definition of flight parameters for analysis

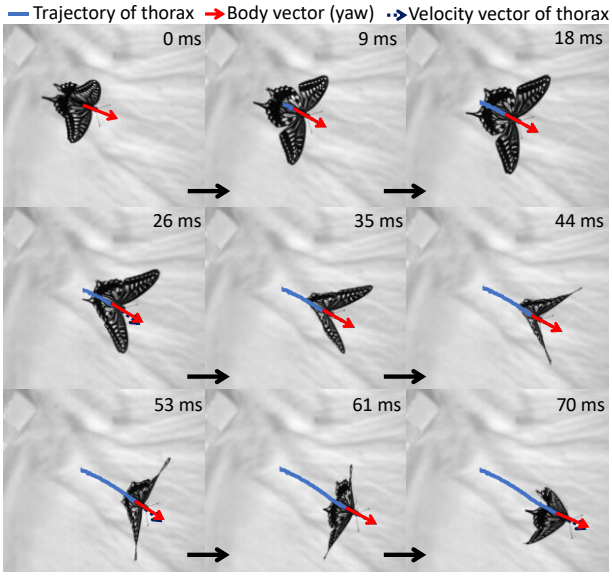

Figure 3. Stroboscopic photographs of a butterfly: forward flight

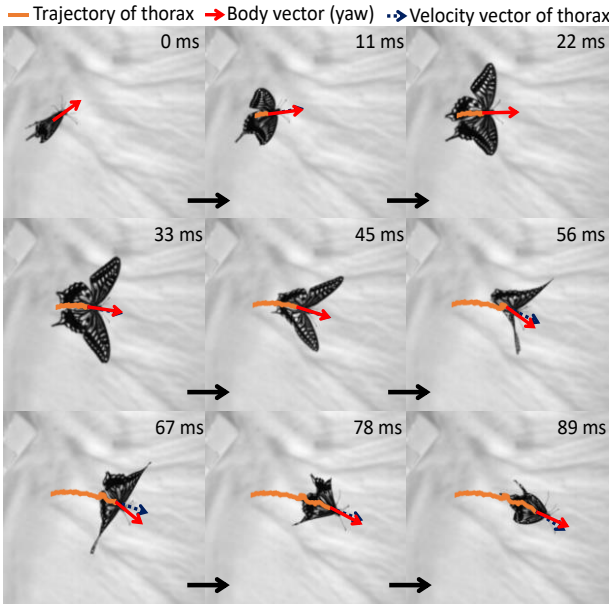

Figure 4. Stroboscopic photographs of a butterfly: turning flight

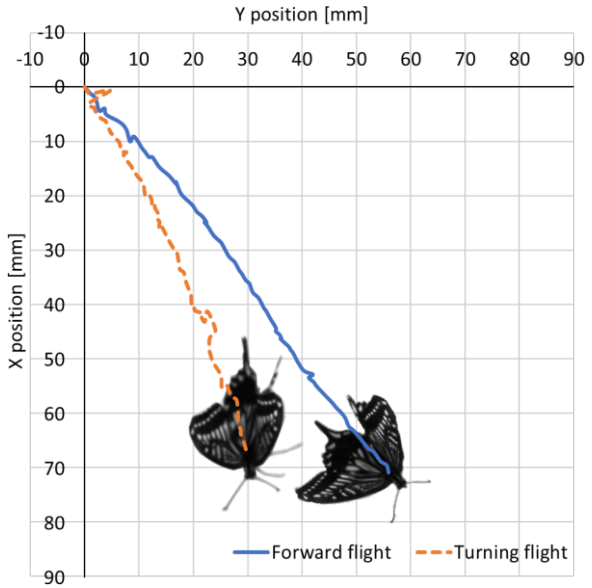

Figure 5. Thorax trajectory of a butterfly as viewed from above the X-Y plane (forward and turning flights)

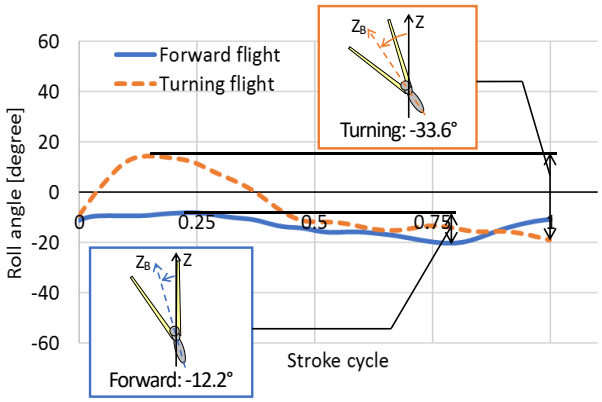

Figure 6. Stroke history of roll angles (forward and turning flights)

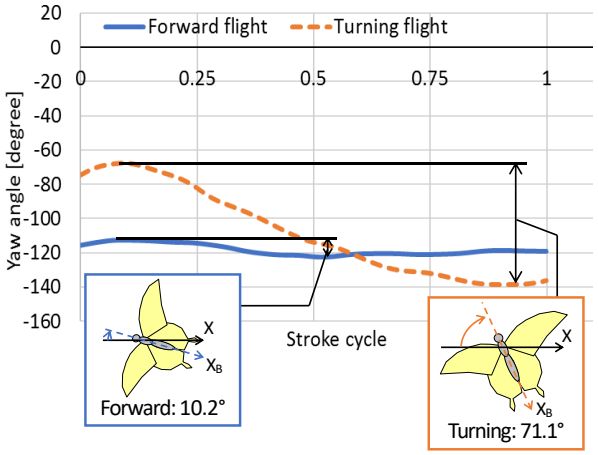

Figure 7. Stroke history of yaw angles (forward and turning flights)

Flights	Radius of curvature [mm] (body length)	Roll angle [degree]	Yaw angle [degree]
Forward 1	-730 (-13.8)	-12.2	-10.2
Forward 2	1481 (28.5)	-13.8	-11.5
Forward 3	1367 (25.8)	-7.8	-6.9
Left turn 1	74 (1.5)	11.2	30.0
Left turn 2	160 (3.5)	14.2	22.5
Left turn 3	56 (1.0)	22.2	64.3
Right turn 1	-52 (-1.0)	-33.6	-71.1
Right turn 2	-79 (-1.3)	-47.1	-70.8
Right turn 3	-242 (4.6)	-13.5	-28.4

Table 2. Relationship between the radius of curvature and roll and yaw angles of butterflies (forward and turning flights)

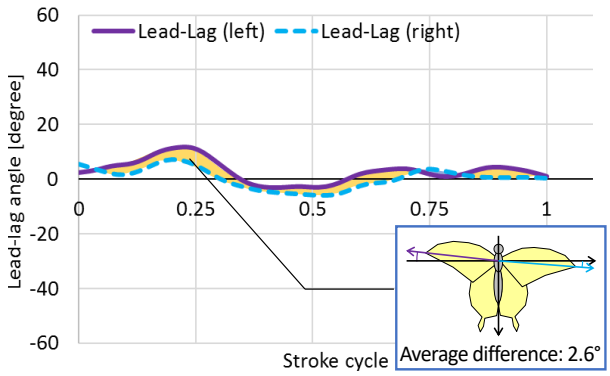

Figure 8. Stroke history of lead-lag (left) and lead-lag (right) angles during forward flight

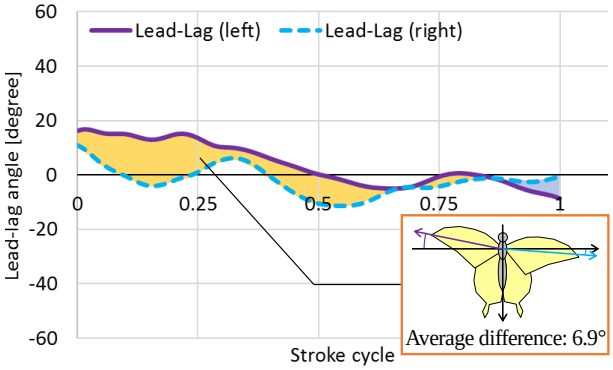

Figure 9. Stroke history of lead-lag (left) and lead-lag (right) angles during turning flight

Flights	Difference of lead-lag angle [deg]	Larger lead-lag angle
Forward 1	2.6	Left
Forward 2	1.3	Left
Forward 3	3.8	Left
Left turn 1	-7.3	Right
Left turn 2	-1.5	Right
Left turn 3	-4.6	Right
Right turn 1	6.9	Left
Right turn 2	12.7	Left
Right turn 3	12.9	Left

Table 3. The obtained lead-lag angles of butterflies (forward and turning flights)

3 MOTION ANALYSIS OF TURNING MECHANISM

3.1 *Parameters of flapping robot*

Figure 10 shows the fabricated flapping robot, which has a wingspan of 120 mm, a forewing cord of 30 mm, a hind wing cord of 60 mm, and a total mass of 505 mg. The robot body and the wing veins were fabricated from bamboo and the wing membrane is 2 μm thick polyethylene film. Four wings were driven by one DOF, i.e., a rubber motor with high power density. A simple slider-crank mechanism and elastic links were used to realize the large flapping motion [Fujikawa 2010]. In this flapping mechanism using a rubber motor, the actuator rotates only in one direction during flight. Here, to investigate the effect by the rotational direction of the actuator and to demonstrate the turning flight by the asymmetric wings, we fabricated three types of flapping robot and set four models (Table 4) for two cases of experiment (Table 5). Figure 11 illustrates a schematic diagram of the actuator rotation as viewed from rear of flapping robot. Models A and B have symmetric wings. Model A rotates the rubber motor counter clockwise, whereas Model B rotates it clockwise. On the other hand, Models AL and AR have asymmetric wings. Model AL rotates the rubber motor counter clockwise and has a swept-forward angle of 10° for the left forewing, whereas Model AR rotates it counter clockwise and has a swept-forward angle of 10° for the right forewing. Note that this swept-forward angle of 10° was set to prevent the shortage of lift by losing the overlap between the fore and hind wings and generating the clearance gap. Case 1 investigates the relationship between the straightness and the rotational direction of the actuator using Models A and B. Case 2 investigates the relationship between the turning flight and the asymmetry of the left and right swept-forward angles using Models A, AL, and AR and verifies the feasibility of steering control using the swept-forward angle.

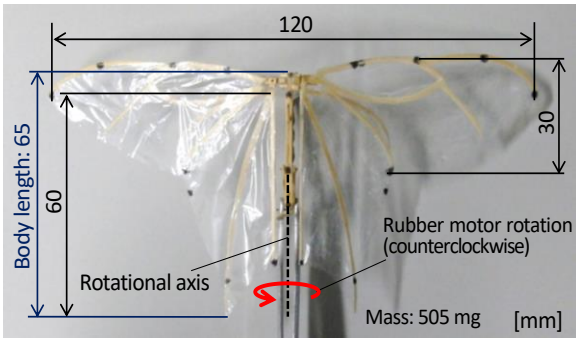

Figure 10. Fabricated flapping robot

Models	Rotational direction	Swept-forward angle [degree]		
		Left	Right	Symmetry
A	Counterclockwise	0	0	Sym.
B	Clockwise	0	0	Sym.
AL	Counterclockwise	10	0	Asym.
AR	Counterclockwise	0	10	Asym.

Table 4. Specification of flapping robot

Experimental cases	Models for comparison
Case 1	Models A and B
Case 2	Models A, AL, and AR

Table 5. Experimental cases

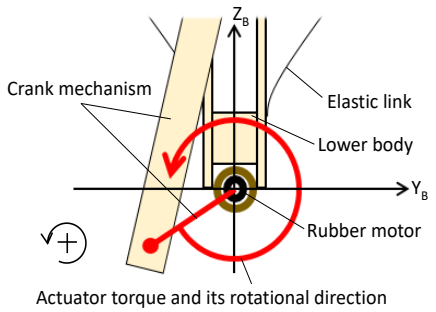

Figure 11. Definition of the actuator rotation as viewed from the rear

3.2 *Case 1: Characteristics for rotational direction of the actuator*

We performed three flight experiments for Case 1 using Models A and B. Figure 12 shows the average thorax trajectory on the X-Y plane and Figs. 13 and 14 indicate the stroke histories of the average roll and yaw angles. The average radii of curvature of Models A and B were 791 mm (12.2 body length) and -712 mm (-11.0 body length), respectively. The radii of curvature were approximately bilaterally symmetric. The roll angles of Models A and B varied by 7.1° and -11.5°, respectively, whereas the yaw angles varied by 3.8° and -10.3°, respectively (Figs. 13 and 14). The transition tendencies of the yaw and roll angles for Models A and B were similar qualitatively and were relatively symmetric with respect to the 0° line. The reason is the influence of the load torque of the actuator at the top and bottom dead points by the slider-crank mechanism. The large instantaneous load torque caused by the bending and twisting of the elastic link stopped the crank motion at the top and bottom dead points and simultaneously the reaction torque rotated the flapping robot inversely.

Based on these results, we found that the rotational direction of the actuator affected the posture, especially, the roll and yaw angles. Hence, counterclockwise rotation of the actuator (Model A) changes the roll posture in the positive direction (counterclockwise) and the yaw posture in the positive direction (counterclockwise), whereas clockwise rotation of the actuator (Model B) changes the roll posture in the negative direction (clockwise) and the yaw posture in the negative direction (clockwise). Note that we define these postures normalized in consideration of this rotational effect as the reference angles (0°) for the following discussion.

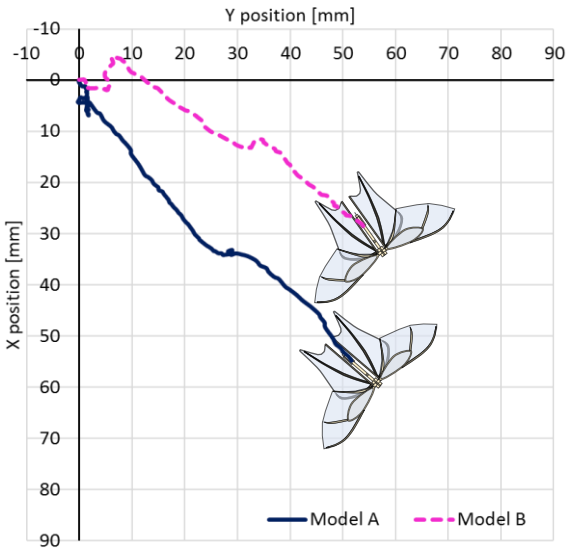

Figure 12. Thorax trajectory of the flapping robot as viewed from above the X-Y plane (Models A and B)

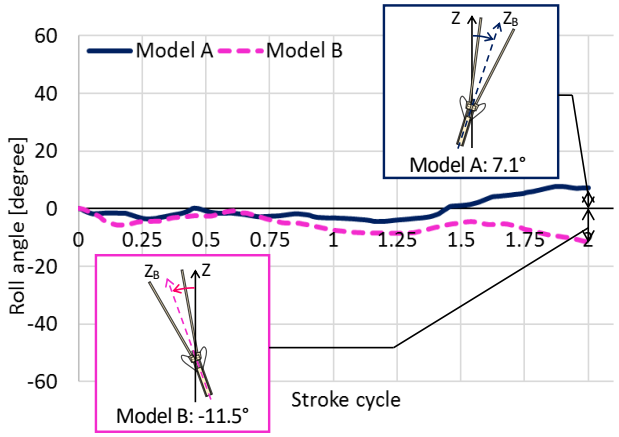

Figure 13. Stroke history of roll angles (Models A and B)

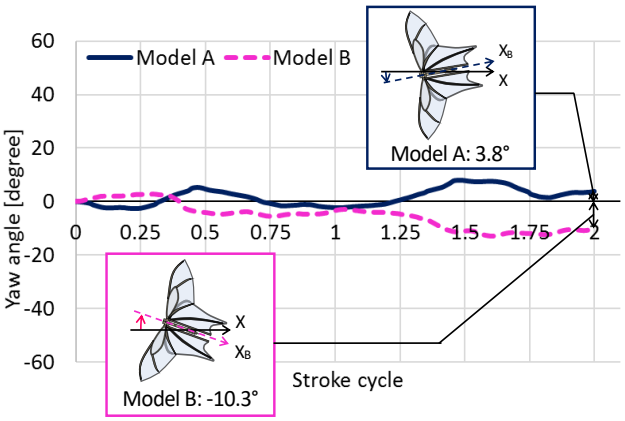

Figure 14. Stroke history of yaw angles (Models A and B)

3.3 Case 2: Characteristics for asymmetric swept-forward angles

We performed three flight experiments for Case 2 using Models A, AL, and AR. Figures 15 and 16 show stroboscopic images (as viewed from above the X-Y plane) of Models AL and AR, respectively. The trajectory of the thorax, the body vector, and the velocity vector indicate that these models first changed their yaw posture and then gradually changed their traveling direction, as was the case for the turning flight of the butterfly. Figure 17 shows the average thorax trajectory on the X-Y plane and Figs. 18, 19, and 20 indicate the stroke histories of average roll, yaw, and pitch angles, respectively. The thorax trajectories of Models AL and AR tended to shift to the right and left, respectively, of the trajectory Model A. The average radii of curvature of Models AL and AR were -235 mm (-3.6 body length) and 175 mm (2.7 body length), respectively, i.e., not symmetric. The reason is due to the mechanism of the actuator rotational direction mentioned above. The roll angles of Models AL and AR shifted to the negative (-20.7°) and positive (16.8°) directions from the reference roll angle of Model A (Fig. 18). The yaw angles of Models AL and AR also shifted to the right (-26.2°) and left (31.3°) from the reference yaw angle of Model A (Fig. 19). From the results in Cases 1 and 2, the effect due to the asymmetric swept-forward angles for the posture was 2 to 4 times bigger than the effect of the rotational direction of the actuator. The asymmetric swept-forward angles changed the balance of reaction force between left and right wings, generated the roll and yaw moments for the center of mass, and chenged the posture. The flapping robot changed periodically the pitch angle with the nose up and nose down motions during the flight (Fig. 20) and hence switched the upward and foreward flights. We believe that this pitch posture control affects the roll and pitch posture strongly and the combination among three angles is one of the important factors of turning flight. To cralify this mechanism quantitatively, we need to visualize and analyze the magnitude and position of reaction forces on the wings.

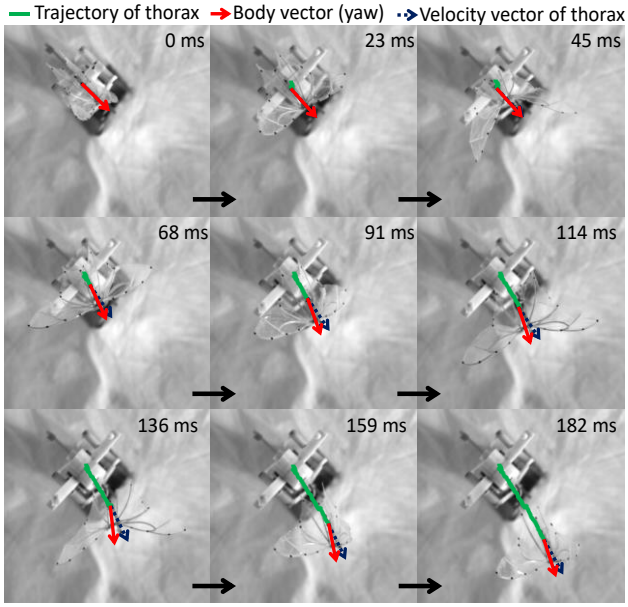

Figure 15. Stroboscopic photographs of the flapping robot: Model AL

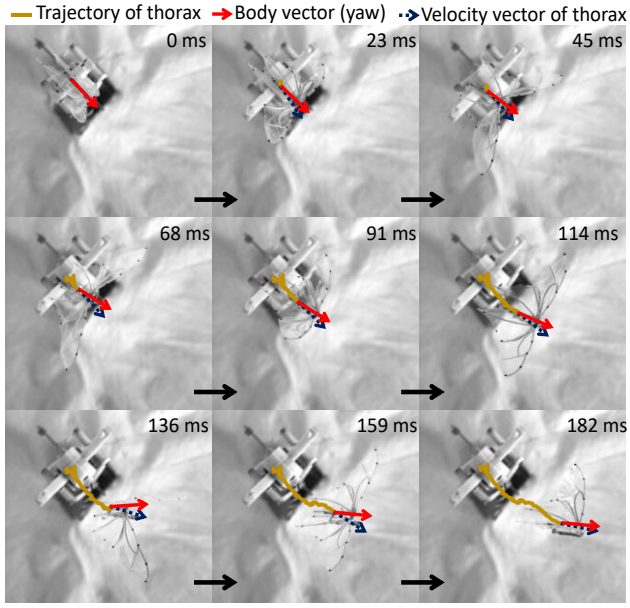

Figure 16. Stroboscopic photographs of the flapping robot: Model AR

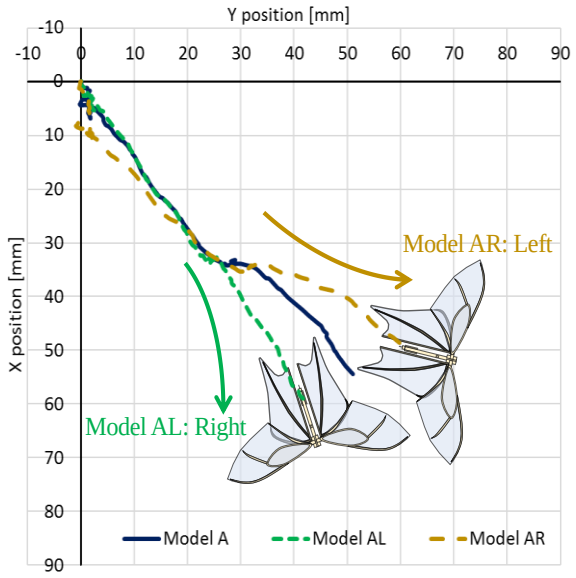

Figure 17. Thorax trajectory of the flapping robot as viewed from above the X-Y plane (Models A, AL, and AR)

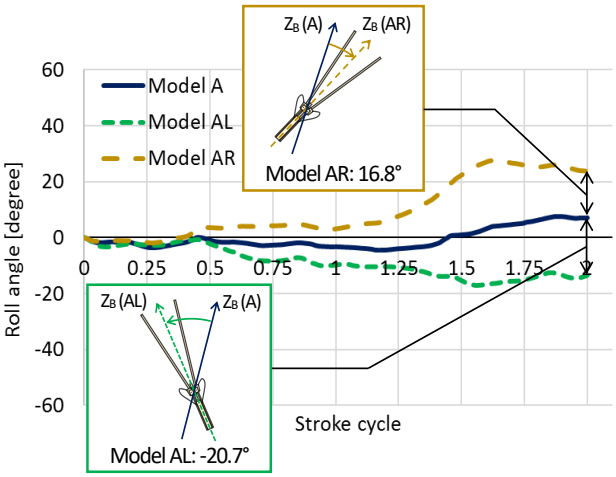

Figure 18. Stroke history of roll angles (Models A, AL, and AR)

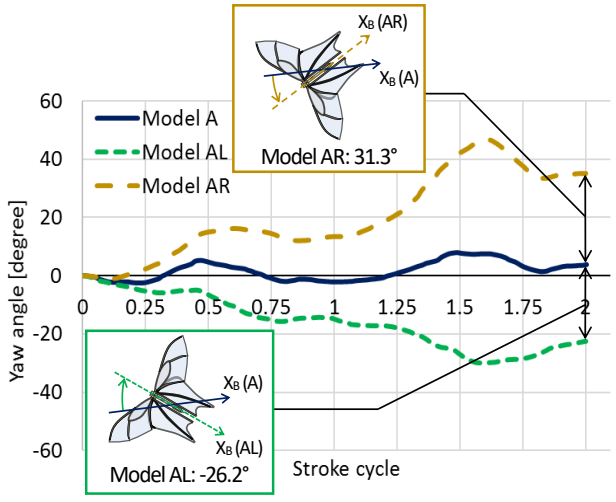

Figure 19. Stroke history of yaw angles (Models A, AL, and AR)

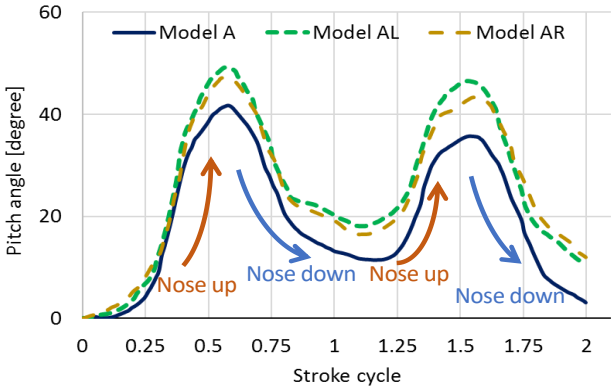

Figure 20. Stroke history of pitch angles (Models A, AL, and AR)

4 CONCLUSIONS

In this study, to realize turning flight in a flapping robot, we analyzed the turning flight of a butterfly and performed the turning flight experiment using flapping robots based on flight analysis results. The flight analysis of a butterfly revealed that the radius of curvature of the turning flight was 110 mm (2.1 body length) and that the turning flight was generated by the combination of the roll and yaw postures. In addition, a butterfly had the difference between the left and right lead-lag angles during the turning flight. Based on these results, we fabricated three types of flapping robot and set four models with the different rotational direction of an actuator and the asymmetric swept-forward angles of 10°. The experimental results showed that the rotational direction of the actuator affected the posture and varied the roll angle by 9.3° and the yaw angle by 7.1°, even if the wings were symmetric. On the other hand, the asymmetric swept-forward angles changed the balance of the reaction force between left and right wings, generated the roll and yaw moments about the robot's center of mass, and caused the body to turn. The roll and yaw angles changed by 18.8° and 28.8°, respectively, during two strokes and the change exceeded the effect by the rotational direction of the actuator.

In the future work, we intend to clarify the turning mechanism by visualizing and analyzing the change of reaction force, pressure, and flow lines generated by the asymmetric swept-forward angles.

REFERENCES

[Fujikawa 2009] Fujikawa, T., et al. Motion Analysis of Butterfly-style Flapping Robot for Different Wing and Body Design. Proceedings of the IEEE International Conference on Robotics and Biomimetics, Thailand, 22-25 February, 2009. Bangkok: IEEE, pp 216-221. ISBN 978-1-4244-2678-2, DOI 10.1109/ROBIO.2009.4913006

[Fujikawa 2010] Fujikawa, T. et al. Development of a Lead-Lag Mechanism Using Simple Flexible Links for a Small Butterfly-Style Flapping Robot. Proceedings of the World Automation Congress, Japan, 19-23 September, 2010. Kobe: IEEE. ISBN 978-1-889335-42-1

[Hsiao 2012] Hsiao, F, Y. et al. Autopilots for Ultra Lightweight Robotic Birds- Automatic Altitude Control and System Integration of a Sub-10 g Weight Flapping-Wing Micro Air Vehicle. IEEE Control Systems, October 2012, Vol. 32, No. 5, pp 35-48. ISSN 1066-033X, DOI 10.1109/MCS.2012.2205475

[Hu 2009] Hu, Z. et al. Aerodynamics of Dragonfly Flight and Robotic Design. Proceedings of the IEEE International Conference on Robotics and Automation, Japan, 12-17 May,

2009. Kobe: IEEE, pp 3061-3066. ISBN 978-1-5090-6893-7, DOI 10.1109/ROBOT.2009.5152760

[Karasek 2016] Karasek, M. et al. Free Flight Force Estimation of a 23.5 g Flapping Wing MAV Using an On-board IMU. Proceedings of IEEE/RSJ International Conference on Intelligent Robots and Systems, South Korea, 9-14 October, 2016. Daejeon: IEEE, pp 4963-4969. ISBN 978-1-5090-3762-9, DOI 10.1109/IROS.2016.7759729

[Lui 2012] Lui, H. et al. Aerodynamics and Flight Stability of a Prototype Flapping Micro Air Vehicle. Proceedings of the ICME International Conference on Complex Medical Engineering, Japan, 1-4 July, 2012. Kobe: IEEE, pp 657-662. ISBN 978-1-4673-1617-0, DOI 10.1109/ICCME.2012.6275676

[Shindo 2014] Shindo, M. et al. Analysis of Roll Rotation Mechanism of a Butterfly for Development of a Small Flapping Robot. American Transactions on Engineering & Applied Sciences, October 2014, Vol. 3, No. 4, pp 233-250. ISSN 2229-1652

[Udagawa 2005] Udagawa, T. et al. Development of a Small-Sized Flapping Robot. Proceedings of the JSDE the 1st International Conference on Design Engineering and Science, Austria, 28-31 October, 2005. Vienna: JSDE, pp 283-288.

[Wood 2008] Wood, R, J. The First Takeoff of a Biologically Inspired At-Scale Robotic Insect. IEEE Transactions on Robotics, April 2008, Vol. 24, No. 2, pp 341-347. ISSN 1552-3098, DOI 10.1109/TRO.2008.916997

[Yokoyama 2008] Yokoyama, T. et al. Development of a Variable-Wing Mechanism based on Flapping Motion of Birds. Proceedings of the SICE Annual Conference, Japan, 20-22 August, 2008. Tokyo: IEEE, pp 168-173. ISBN 978-4-907764-30-2, DOI 10.1109/SICE.2008.4654643

CONTACTS:

Mr. Yuta Ozawa
Chiba Institute of Technology
Department of Advanced Robotics,
2-17-1, Tsudanuma, Narashino, Chiba, 275-0016, JAPAN
e-mail: kikut@ieee.org
http://www.kikulab.it-chiba.ac.jp